The Inverse Autotransporter Intimin Exports Its Passenger Domain via a Hairpin Intermediate*

Philipp Oberhettinger[‡], Jack C. Leo[§], Dirk Linke[§], Ingo B. Autenrieth[‡], and Monika S. Schütz[‡1]

From the [‡]Institut für Medizinische Mikrobiologie und Hygiene, Universitätsklinikum Tübingen, Elfriede-Aulhorn-Strasse 6, 72076 Tübingen, Germany and the [§]Department of Biosciences, University of Oslo, P.O. Box 1066 Blindern, 0316 Oslo, Norway

Background: Intimin exports its C-terminal passenger domain through an N-terminal β-barrel onto the bacterial surface.
Results: Insertion of an epitope tag at the very N terminus of the passenger domain stalls the export of the passenger.
Conclusion: The intimin passenger adopts a hairpin conformation during translocation.
Significance: Our results confirm the hairpin model of inverse autotransport where the passenger is translocated from the N to the C terminus.

Autotransporter proteins comprise a large family of virulence factors that consist of a β-barrel translocation unit and an extracellular effector or passenger domain. The β-barrel anchors the protein to the outer membrane of Gram-negative bacteria and facilitates the transport of the passenger domain onto the cell surface. By inserting an epitope tag into the N terminus of the passenger domain of the inverse autotransporter intimin, we generated a mutant defective in autotransport. Using this stalled mutant, we could show that (i) at the time point of stalling, the β-barrel appears folded; (ii) the stalled autotransporter is associated with BamA and SurA; (iii) the stalled intimin is decorated with large amounts of SurA; (iv) the stalled autotransporter is not degraded by periplasmic proteases; and (v) inverse autotransporter passenger domains are translocated by a hairpin mechanism. Our results suggest a function for the BAM complex not only in insertion and folding of the β-barrel but also for passenger translocation.

Gram-negative bacteria evolved numerous secretion systems to transport proteins across the two membranes surrounding the bacterial cytoplasm. One of these systems is the so-called type V secretion (1, 2), representing monomeric (type Va) (3, 4) and trimeric autotransporters (type Vc) (5), two-partner secretion (type Vb) (6), and the patatin-like protein PlpD (type Vd) (7). Recently, a new family of proteins, the type Ve secretion system, was described (2, 8). Two prominent members of that family are invasin of enteropathogenic *Yersinia* strains (9) and intimin of enteropathogenic *Escherichia coli* strains (10, 11). Both are adhesins mediating binding to host cells and are therefore important virulence factors. Members of this family consist of an N-terminal signal peptide (12), a short periplasmic domain (13, 14) followed by a 12-stranded β-barrel pore, and a

C-terminal passenger domain consisting of several Ig domains. This represents an inverse domain order compared with classical monomeric autotransporters, which have a C-terminal β-barrel domain anchoring the protein to the outer membrane (2, 13). After synthesis in the cytosol, autotransporters of type Ve are transported into the periplasm by the Sec translocon, guided through the periplasm by chaperones like SurA, and finally inserted into the outer membrane via the BAM complex (8, 15, 16).

Several models try to explain the export of the passenger domain of classical monomeric autotransporters (type Va) onto the bacterial surface; according to the threading model, the N terminus is transported first through the β-barrel pore (17), whereas in the hairpin model, the C-terminal part of the passenger domain forms a hairpin structure. Then folding of the passenger on the bacterial surface drives the translocation of the rest of the protein (18, 19). However, the necessity of additional energy sources has been discussed (20, 21). Another model suggests the involvement of the BAM complex not only in the insertion of the β-barrel domain of autotransporters but also in the export of the passenger domain to the cell surface. This model is supported by studies in which the passenger domain of autotransporter intermediates was cross-linked to BamA (22, 23) as well as by the finding that even some folded polypeptides might be transported to the cell surface (24). In this study, we created a stalled type Ve autotransporter intermediate of the adhesin intimin of enteropathogenic *E. coli* (EPEC)[2] O127:H6 by inserting a double HA tag after amino acid position 453. This position is located in the D00 domain, which comprises the N-terminal part of the extracellular passenger domain (Fig. 1A) (25). The D00 is a protease-resistant domain with unknown function. Because the D00 is neither a bacterial immunoglobulin-like nor a C-type lectin domain, an important role in passenger domain translocation or intimin dimerization was assumed (13, 25). With the help of this mutant, we were able to show that the β-barrel domain appears to be folded and stably inserted into the bacterial outer membrane, although the export of the passenger domain to the cell surface is not com-

---

[1] To whom correspondence should be addressed: Institut für Medizinische Mikrobiologie und Hygiene, Universitätsklinikum Tübingen, Elfriede-Aulhorn-Str. 6, 72076 Tübingen, Germany. Tel.: 49-7071-81527; Fax: 49-7071-295440; E-mail: monika.schuetz@med.uni-tuebingen.de.

[2] The abbreviations used are: EPEC, enteropathogenic *E. coli*; PK, Proteinase K; DSP, dithiobis(succinimidylpropionate).

TABLE 1
Strains and plasmids used in this study

Name	Relevant genotype or description	Reference/Source
E. coli **strains**		
EPEC O127:H6	Enteropathogenic *E. coli* O127:H6 strain 2348/69	Ref. 50
EPEC O127:H6 Δ*eaeA*	Enteropathogenic *E. coli* O127:H6 strain 2348/69, Δ*eaeA*	Provided by Prof. Gad Frankel (London, UK)
E. coli BL21(DE3)omp2	BL21 (DE3), *ompF*::*Tn5*, Kan^R	Ref. 51
Plasmids		
pASK-IBA2	Expression vector with AHTC inducible promoter, Amp^R	IBA Technologies
pASK-IBA2_*eaeA*	*eaeA* gene in XbaI-HindIII sites of pASK-IBA2, Amp^R	Ref. 8
pASK-IBA2_*eaeA*-HA derivative	IntHA453 in XbaI-HindIII sites of pASK-IBA2 with a tandem HA tag after residue 453, Amp^R	This study
pASK-IBA2_*eaeA*-StrepTag II derivatives	Int WT and IntHA453 in XbaI-HindIII sites of pASK-IBA2 with C-terminal Strep-tag, Amp^R	This study

pleted yet. In addition, we could identify transient interaction partners, and by different approaches, we were able to confirm that the transport of the passenger domain occurs by adopting a hairpin conformation, suggesting that hairpin formation might be a general feature of all type V secretion systems possibly with the exception of two-partner secretion.

EXPERIMENTAL PROCEDURES

Bacterial Strains and Growth Conditions—*E. coli* BL21(DE3)-omp2 was transformed with pASK-IBA2 expression vectors containing wild type or mutant *eaeA,* respectively. The strains were grown at 27 °C in soy broth supplemented with a piece of autoclaved bovine liver and 100 μg/ml ampicillin (Applichem). Overnight cultures were diluted into fresh medium to an A_{600} of 0.1. Bacterial cultures were then subcultured for 2 h at 27 °C before anhydrotetracycline (IBA GmbH) was added at a final concentration of 200 ng/ml. To record growth curves, the A_{600} was determined every 30 min. If not stated otherwise, bacteria were then allowed to express wild type or mutant EaeA for another 2 h. The E2348/69 Δ*eaeA* EPEC strain was grown at 37 °C in LB medium. A list of all bacterial strains used in this study is given in Table 1.

Site-directed Mutagenesis—To exchange single amino acids in the intimin protein providing amber mutants, site-directed mutagenesis was used. A pair of complementary primers, both including the appropriate nucleotide sequence to yield the desired amino acid, were used for PCR. The derived PCR product was directly used for transformation into competent *E. coli* DH5α. The sequence of the resulting plasmid was verified as correct by DNA sequencing.

Cloning and Generation of Intimin Constructs—Intimin WT and IntHA453 mutant were constructed and cloned as described previously (8). Two C-terminal Strep-tags (GSG-SAWSHPQFEK-GSG-SAWSHPQFEK) were introduced by PCR and verified by DNA sequencing. A list of all plasmids used in this study is given in Table 1.

Protease Digestion and Protein Precipitation—2×10^8 intimin-expressing bacteria were washed once, resuspended in PBS containing 50 μg/ml Proteinase K (Thermo Scientific), and incubated for 30 min on ice. To stop digestion, 4 mM phenyl-methylsulfonyl fluoride (PMSF) was added. To separate proteins that were released into the supernatant by Proteinase K (PK) digestion, bacteria were centrifuged for 5 min at 5000 $\times$ *g*, and the cleared supernatant was transferred into a new tube. Subsequently, proteins were precipitated by methanol and chloroform. Therefore, the sample volume was adjusted to 400 μl, and an equal volume of methanol as well as 300 μl of chloroform were added. After centrifugation at 13,000 rpm for 5 min, supernatant was rejected, and 300 μl of methanol was appended to the remaining protein interphase. After an additional centrifugation step, the pellet was resuspended in SDS buffer. The samples were boiled for 10 min at 95 °C and analyzed by SDS-PAGE and Western blot.

Subcellular Fractionation—50 ml of bacteria expressing intimin WT or intimin variants were collected by centrifugation (4500 $\times$ *g*, 5 min). After a washing step of the pellet, bacteria were resuspended in 500 μl of resuspending buffer (0.2 M Tris-HCl, pH 8.0, 1 M sucrose, 1 mM EDTA, 1 mg/ml lysozyme) with protease inhibitor (Roche Applied Science) and incubated for 5 min at room temperature. Afterward, 3.2 ml of H_2O was added for 5 min, and the spheroblasts were centrifuged for 45 min at 200,000 $\times$ *g*. The supernatant containing the periplasmic fraction was transferred into a new tube. The pellet was resuspended in French Press buffer (10 mM Tris-HCl, pH 7.5, 5 mM EDTA, 0.2 mM DTT, 1 μl DNase I (1 mg/ml), 1 mM MgCl$_2$), and cells were disrupted by the French Press. Remaining intact cells were separated by centrifugation. The cleared supernatant was ultracentrifuged for 1 h at 290,000 $\times$ *g*. The supernatant with the cytosolic proteins was transferred into a clean tube again, and the pellet containing the membranes was resuspended in H_2O.

Cross-links with Dithiobis(succinimidylpropionate) (DSP)—Two hours after induction of intimin expression, 50 ml of bacterial cells were harvested, washed once with PBS, and finally resuspended in 2.5 ml of PBS with 0.5 mM cross-linker DSP. The suspension was incubated for 30 min at room temperature on a rocking shaker and subsequently quenched with 40 mM Tris-HCl (pH 7.4). After centrifugation, outer membranes were prepared as described. For solubilizing the proteins, membrane pellets were resuspended in freshly prepared 20 mM Tris-HCl (pH 8), 0.3 M NaCl, 0.5% *n*-dodecyl β-D-maltoside-containing buffer and incubated overnight at 4 °C. After a 30-min centrifugation step (TLA55, 55,000 rpm), 100 μl of streptactin super-flow suspension was added to the supernatant for an additional 2 h. After three washing steps with buffer containing 100 mM Tris-HCl (pH 8), 150 mM NaCl, 1 mM EDTA, 0.1% *n*-dodecyl β-D-maltoside, proteins were eluted with 2.5 mM desthiobiotin and SDS sample buffer.

Sample Preparation for Western Blot Analysis—For preparation of whole cell lysates, bacterial pellets were resuspended in H_2O and SDS sample buffer to obtain 5×10^6 bacteria/ml and incubated for 10 min at 95 °C before loading on the gel.

Western Blot Analysis—Proteins resolved by SDS-PAGE were transferred onto nitrocellulose membranes. The membranes were blocked overnight with TBS/T (5 mM Tris-HCl, 138 mM NaCl, 0.1% Tween 20, pH 8.0) plus 5% milk powder (w/v) at 4 °C. Blots were probed with purified IgG fraction of polyclonal rabbit anti-EaeA (1:5000), anti-BamA-E (1:5000), anti-SurA (1:5000), anti-Skp (1:5000), anti-MBP (1:1000), anti-GyrA (1:1000), guinea pig anti-DegP (1:1000), monoclonal mouse anti-HA tag, anti-Strep-tagII, or anti-His tag and a peroxidase-conjugated secondary anti-rabbit (diluted 1:10,000; Dianova, Hamburg, Germany), anti-mouse (diluted 1:1000; Dako, Denmark), or anti-guinea pig antibody (diluted 1:5000; Dianova). Anti-BamA and -EaeA sera had been preadsorbed against paraformaldehyde-fixed bacteria deficient in the respective antigen before. As a molecular weight marker, a PageRuler unstained protein ladder (Thermo Scientific) was used.

Preparation of Outer Membrane Fractions—Preparation of outer membranes was carried out using 50 ml of bacterial culture. Cells were harvested and resuspended in 500 μl of resuspension buffer (0.2 M Tris, 1 M sucrose, 1 mM EDTA, pH 8). After the addition of 500 μg of lysozyme (20 units/μg; MSB) and 3.2 ml of water, the samples were incubated for 20 min at room temperature. Protoplasts were lysed in 5 ml of lysis buffer (2% Triton X-100, 50 mM Tris, 10 mM MgCl$_2$, pH 8), and released DNA was digested by the addition of 50 μg of DNase I (10 mg/ml; Roche Applied Science). Outer membranes were pelleted by centrifugation at 85,000 $\times$ g for 60 min at 4 °C. After three washing steps with water, the membranes were resuspended in SDS sample buffer. The protein profile of abundant outer membrane proteins was visualized by staining SDS gel with Coomassie Brilliant Blue (Bio-Rad) for 1 h, followed by discoloration and recording using the Odyssey imaging system (LI-COR Biosciences).

Urea Extraction of Outer Membrane Preparations—Bacterial envelopes were pelleted by ultracentrifugation at 290,000 $\times$ g for 1 h. The membranes were resuspended in 1 ml of urea solution (100 mM glycine, 6 M urea, 15 mM Tris-HCl, pH 7.4) and extracted for 1 h at 37 °C. Membranes from urea-treated samples were reisolated by centrifugation at 290,000 $\times$ g for 90 min at 25 °C and resuspended in SDS sample buffer.

Immunofluorescence Microscopy—For immunofluorescence stainings, 2×10^7 bacteria in PBS were centrifuged on polyethyleneimine-coated coverslips, fixed for 30 min with 4% paraformaldehyde in PBS (w/v), and subsequently blocked with 1% bovine serum albumin (BSA) in PBS (w/v) at room temperature. For stainings of periplasmic localized antigens, bacterial cell walls were permeabilized for 20 min in 0.5% Triton X-100 plus PBS (v/v). Stainings were performed using preadsorbed polyclonal rabbit antibodies directed against EaeA (provided by Prof. Gad Frankel, London, UK) (26) (diluted 1:200) and a 1:200 dilution of a Cy2-conjugated secondary anti-rabbit antibody (Dianova). Strep-tagII (diluted 1:100) or HA tag (diluted 1:100) was stained with corresponding monoclonal mouse antibodies and Cy3-conjugated secondary anti-mouse antibody in a 1:100 dilution (Dianova). Secondary antibodies were incubated at room temperature for 2 h in a dark chamber. Finally, coverslips were mounted with Mowiol. Fluorescence images were obtained using an upright Leica DMRE fluorescence microscope (Leica, Wetzlar, Germany) equipped with a Leica black and white digital camera using the $\times$100 objective, optovar $\times$1.6, and the software Leica application suite. All samples within one experiment were recorded at identical software settings (exposure, γ correction). Images were processed and assembled into figures using Adobe Photoshop.

Quantification of Intimin Surface Localization by Flow Cytometry—Two hours after the start of intimin protein expression, 5×10^7 bacteria were harvested by centrifugation. Cells were washed with PBS, fixed with 4% paraformaldehyde, and finally blocked with 1% BSA in PBS. Afterward, cells were stained with rabbit anti-intimin (1:200), mouse anti-HA tag, or mouse anti-Strep-tag antibodies overnight at 4 °C followed by an incubation with anti-rabbit Cy2- (1:100; Dianova) or anti-mouse Dylight649-conjugated (1:100; Jackson, Newmarket, UK) secondary antibody for 2 h at room temperature. Surface localization of intimin C-terminal domain, HA tag, or Strep-tag was measured by flow cytometry using an LSRFortessa cell analyzer (BD Biosciences). Data were analyzed with WinMDI (J. Trotter) software. The mean fluorescence intensity of three independent experiments is shown.

Intimin Adhesion Assay—1.5×10^5 HeLa cells (ATCC number: CCL-2) were seeded onto coverslips and grown overnight in RPMI 1640 (Biochrom, Berlin, Germany) supplemented with 10% fetal calf serum (FCS) (Invitrogen) and 1% penicillin/streptomycin. The next day, cells were washed twice and incubated in medium without antibiotics at 37 °C and 5% CO$_2$ for 1 h before preinfection with *E. coli* E2348/69 Δ*eaeA* EPEC strain (provided by Prof. Gad Frankel, London, UK). Overnight cultures of the EPEC *eaeA* mutant strain were subcultivated for 2 h at 37 °C, harvested by centrifugation (4000 $\times$ g, 5 min), and washed once with PBS. Then HeLa cells were infected at a multiplicity of infection of 100. Bacteria were centrifuged onto the cells at 300 $\times$ g for 2 min and incubated for 2 h at 37 °C in 5% CO$_2$ followed by four washing steps. Remaining adherent bacteria were killed by incubation with gentamicin (100 μg/ml) for 1 h. Finally, cells were washed with medium without antibiotics. For infection with *E. coli* BL21(DE3)omp2 strains expressing the wild type or mutant intimin variants, bacteria were subcultivated as described above. After 2 h of protein expression, bacteria were harvested and washed once with PBS. The preinfected HeLa cells were then infected at a multiplicity of infection of 100 for 2 h. Following three washing steps with PBS, the cells were fixed overnight with 4% paraformaldehyde in PBS. After staining of cells with fuchsine for 30 s, the coverslips were finally mounted in Entellan (Merck) and analyzed with a light microscope with $\times$100 magnification.

RESULTS

Insertion of a 2$\times$ HA Tag after Amino Acid 453 into the Intimin Passenger Domain Abolishes Adhesion to Tir-primed HeLa Cells—In a previous study (8), we analyzed the topology of the intimin membrane anchor by insertion of tandem HA epitope tags into (i) loops and turns, (ii) the periplasmic domain at the N terminus, (iii) the α-helical linker between β-barrel and passenger domain, and (iv) the passenger domain. By the insertion of a tandem HA epitope tag (Fig. 1*A*) after amino acid 453 into the passenger domain of intimin (IntHA453), we created
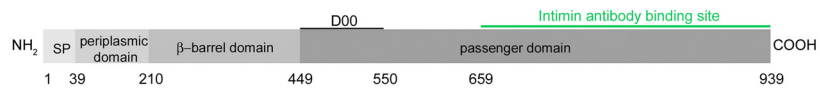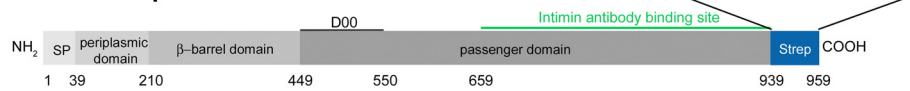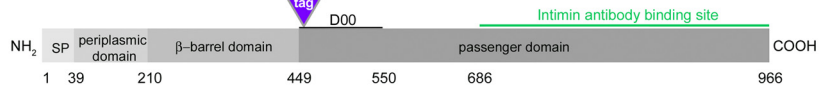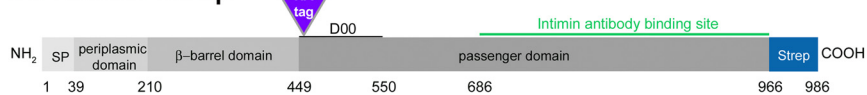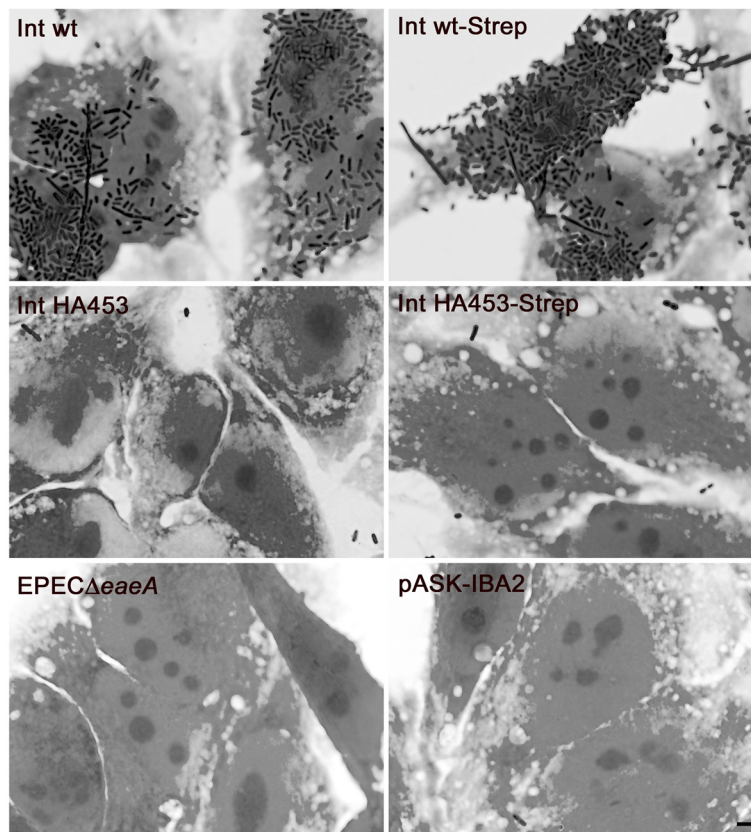
ASBMB

FIGURE 1. **IntHA453 is not able to mediate adhesion of *E. coli* to HeLa cells carrying the Tir receptor.** *A*, domains of EPEC intimin. Amino acids comprising the individual domains are depicted, and insertion sites and sequence of the HA tag (*purple*) as well as of the Strep-tag (*blue*) are shown; the intimin antibody binding site is *labeled* in *green*. *B*, HeLa cells were preinfected with EPECΔ*eaeA* that injected the Tir receptor into the host cell membrane. Subsequently, HeLa cells were infected with *E. coli* BL21(DE3)omp2 expressing intimin WT (*Int wt*), the HA-tagged variant IntHA453, and the Strep-tagged version thereof (*Int wt-Strep* and *IntHA453-Strep*). Adhesion is only possible if the C terminus of intimin is correctly folded and exposed on the bacterial cell surface. Proper adhesion was only observed for bacteria expressing Int WT or Int WT-Strep. *Scale bar*, 2 μm.
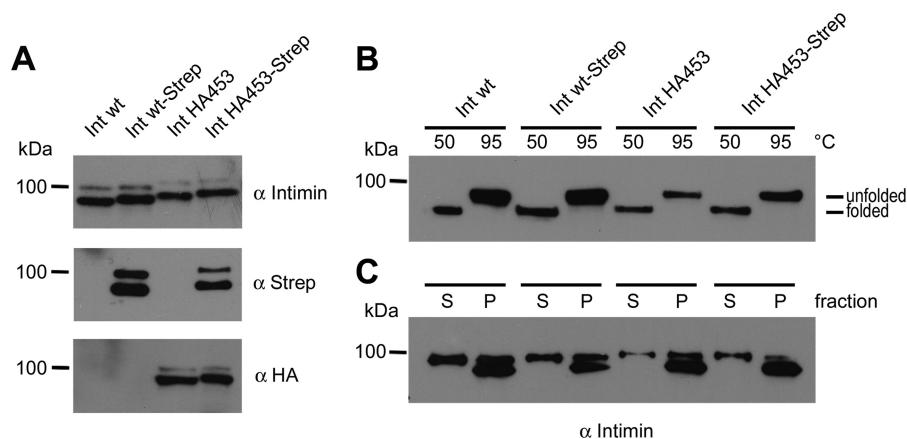
FIGURE 2. **Expression and assembly of wild type intimin and Strep/HA-tagged variants in the bacterial outer membrane.** *A*, expression of intimin constructs in *E. coli* BL21(DE3)omp2 was induced by adding anhydrotetracycline. Protein profiles of whole cell lysates were analyzed by Western blotting and immunodetected with antibodies against intimin, Strep-tag, or HA tag. *B*, heat shift. Correct folding of the β-barrels from intimin WT and intimin variants was analyzed by heating outer membrane fractions at 50 and 95 °C, respectively. Properly folded β-barrels show heat modifiability due to denaturation only at higher temperature. *C*, urea extraction. To distinguish between fully membrane-inserted and loosely attached membrane proteins, outer membrane fractions were incubated with 6 M urea. Afterward, insoluble material (pellet (*P*)) was separated by ultracentrifugation from the supernatant (*S*) containing the soluble protein fraction.

an intimin variant producing an interesting adhesion phenotype (described below). Intimin as an adhesin specifically binds to Tir (translocated intimin receptor). Tir is injected into host cells by EPEC (10, 27) via a type III secretion system. To test the adhesive properties of IntHA453 as a functional readout for surface display of the passenger, we analyzed the ability of IntHA453 to mediate adherence to the Tir receptor. Therefore, HeLa cells were primed with the Tir receptor by an intimin-deficient EPEC strain (EPEC Δ*eaeA*). Using the method established by Oberhettinger *et al.* (8), the same cells were infected with *E. coli* BL21(DE3)omp2 expressing wild type intimin (Int WT), IntHA453, or C-terminally Strep-tagged versions (Fig. 1*A*) thereof. As shown in Fig. 1*B*, bacteria expressing Int WT or Int WT-Strep were able to resist being removed by extensive washing steps, indicating adhesion to the host cells via the Tir receptor. In contrast, bacteria expressing IntHA453 were efficiently removed by washing, which is indicative of weak or no binding. Moreover, our data demonstrate that a C-terminally attached Strep-tag does not disturb *per se* the adhesive properties (and thus passenger translocation) of intimin because we detected comparable numbers of bacteria expressing Int WT or Int WT-Strep binding to Tir-primed cells. As a control for efficient removal of EPEC Δ*eaeA*, which was used for priming the cells with the Tir receptor, HeLa cells that were only preinfected are depicted (EPEC Δ*eaeA*). *E. coli* BL21(DE3)omp2 carrying an empty vector (pASK-IBA2) was included as a negative control for binding to Tir-primed cells. Taken together, our findings indicate that IntHA453 is not able to mediate adhesion of bacteria to host cells carrying the Tir receptor.

IntHA453 Is Expressed at the Wild Type Level and the β-Barrel Domain Appears Folded and Stably Inserted into the Outer Membrane—Above we have shown that IntHA453 is not able to mediate adhesion to Tir-primed HeLa cells. There are at least two possible explanations for this phenotype; because we know that autotransporter-mediated adhesion is very much a dose-dependent effect (28, 29), the protein expression level of IntHA453 might be reduced compared with Int WT. Alternatively, the IntHA453 is expressed at wild type levels, but it is

either masked or misfolded and thus not able to adhere to the Tir receptor. To test these hypotheses, we analyzed the protein expression levels by Western blot, the folding of the β-barrel by heat modifiability assays, and a stable outer membrane insertion by urea extraction. As shown by Western blots with whole cell lysates and by using antibodies directed against the C-terminal part of the passenger domain of intimin (Fig. 2*A*, *top*), the C-terminal Strep-tag (*middle*), or the HA epitope tag (*bottom*), Int WT, Int WT-Strep, IntHA453, and IntHA453-Strep are expressed in comparable amounts. All proteins had an apparent molecular mass of ∼100 kDa, which is in accordance with the calculated molecular weight. We did not observe degradation products with any of the intimin variants. Taken together, our results demonstrate that the expression level of IntHA453 is comparable with that of the wild type and thus is not the cause of the altered adhesion behavior.

In order to examine whether the intimin protein variants are correctly folded and inserted into the lipid bilayer, we first prepared outer membrane fractions of *E. coli* BL21(DE3)omp2 expressing the indicated proteins. Then we performed a heat modifiability experiment, a typical assay to assess the folding of β-barrel proteins (8, 30). As shown in Fig. 2*B*, all intimin variants migrate faster through the SDS gel after heating at 50 °C. This species represents the folded form of the β-barrel. Upon heating to 95 °C, the running behavior is altered due to denaturation of the entire protein. This result is remarkable especially for the IntHA453 mutants, because (i) the inserted tags do not interfere with β-barrel folding, and (ii) the folding of the β-barrel obviously is completed (this will be of interest later on).

In addition to the heat modifiability assay, we tested whether the intimin variants are correctly inserted into the lipid bilayer or only loosely attached to the membrane by weak hydrophobic interactions. Therefore, membrane protein fractions were extracted with 6 M urea, and subsequently the pellet fraction (*P*), containing the fully integrated insoluble proteins, was separated from the supernatant (*S*), containing the extractable proteins. As shown in Fig. 2*C*, the major fraction of the tested

proteins was found in the pellet fraction. A minor fraction of the proteins was extractable by urea, conceivably due to the over-expression conditions we have used. Thus, we can conclude that IntHA453 is folded and inserted into the outer membrane in amounts comparable with Int WT. This indicates that the loss of adhesive properties was not due to reduced assembly efficiency and/or reduced insertion into the outer membrane.

Surface Display of the Passenger Domain Is Impaired in IntHA453—In order to test whether the passenger domain is localized on the cell surface, we performed immunofluorescence experiments. By using an antibody directed against the most C-terminal 280 amino acids (26) (Fig. 1*A*), we are able to detect the intimin passenger only. Moreover, by omitting a permeabilization step prior to the application of the antibody, we can detect the passenger only if it is exposed on the bacterial surface (8). We found that bacteria expressing Int WT or Int WT-Strep showed a ring-shaped outer membrane staining with the anti-intimin antibody (Fig. 3*A*). This finding indicates surface exposure of the passenger domain. However, IntHA453 as well as the Strep-tagged variant thereof (IntHA453-Strep) yielded a significantly reduced fluorescence signal (Fig. 3*A, top*). To our surprise, when we performed the same assay with antibodies directed against the HA epitope tag, we were able to detect it on the bacterial surface (Fig. 3*A, middle*). Neither an unfolded but exported passenger (which would be detected by the Int antibody on the surface) nor degradation of the passenger (which was excluded above) can explain this effect. Thus, we assumed that by inserting the tandem HA tag, we had generated a stalled autotransport intermediate, in which passenger translocation was initiated but the process was interrupted before passenger export was complete. If then transport of the passenger is initiated by the formation of a hairpin, one would be able to detect the HA tag on the bacterial surface but not the C-terminal part of the passenger domain. This hypothesis was supported by the fact that the most C-terminal Strep-tag, which is surface-exposed for Int WT-Strep and which does not interfere with autotransport (Fig. 3*A, bottom*), is not detectable on the cell surface in bacteria expressing IntHA453-Strep. All of these findings were corroborated and quantified by fluorescence-activated cell sorting (FACS) (Fig. 3*B*). From these data, we hypothesized that IntHA453 might be a stalled autotransport intermediate adopting a topology as illustrated in Fig. 3*C*. This intermediate probably arose due to the disruption of the D00 domain of intimin. Position 453 lies within the first predicted β-strand of the N-terminal extracellular domain (D00) of the passenger Thus, the introduced double HA tag presumably leads to misfolding of the D00 domain. Tsai *et al.* (13) assumed that this domain could function as an autochaperone domain as it was described for classical monomeric autotransporters (31–33). Such domains initiate the vectorial export of the passenger by forming a hairpin intermediate and improve transport efficiency. This could explain why the insertion of the double HA tag leads to stalling. However, to confirm this hypothesis, we had to test by other means whether our topology model really holds true.

The C-terminal Part of the Passenger Domain of IntHA453 Can Be Cleaved off of the N-terminal β-Barrel by Proteinase K Treatment but Is Protected from Further Degradation—To analyze the putative autotransport intermediate in more detail and

to characterize the topology of the C-terminal passenger domain, we performed proteolytic treatment with PK. As reported elsewhere (15), Int WT as well as Int WT-Strep are resistant to protease, because PK treatment leads to a slight decrease only in the total amount of protein. Compared with Int WT, IntHA453 was highly sensitive to PK treatment (Fig. 4*A*). Whereas the signal for the full-length protein quantitatively disappeared with IntHA453 and IntHA453-Strep, we could observe the formation of a fragment of about ~55 kDa (referred to hereafter as the PK fragment). The PK fragment was not only detectable with the intimin antibody, indicating that the fragment contains at least parts of the intimin antibody binding site (*i.e.* the passenger domain (depicted in Fig. 1*A*)), but under the chosen experimental conditions, it was also protected from further degradation. Immunofluorescence staining of PK-treated bacteria expressing the intimin variants using the anti-intimin antibody confirmed the protease resistance of Int WT and Int WT-Strep, because the outer membrane still displayed ring-shaped staining. However, IntHA453 and IntHA453-Strep could not be detected on the surface of untreated as well as PK-treated bacteria using the anti-intimin antibody (Fig. 4*B*).

Because the tandem HA tag is intrinsically unfolded, we assumed that it might be the structure that is proteolyzed by PK. To investigate that possibility, we used bacteria producing IntHA453 or IntHA453-Strep and treated them with PK. Then whole cell lysates were prepared and analyzed by Western blot and immunofluorescence staining using antibodies directed against the HA tag. We found that the HA tag was no longer detectable after treatment with PK as detected by Western blotting (Fig. 4*C, left*). Digestion of the HA tag also resulted in a loss of fluorescence signal on the cell surface of *E. coli* (Fig. 4*C, right*). As our intimin antibody recognizes the last 280 amino acids of the C-terminal passenger domain, we assumed that the ~55-kDa fragment, which is detectable with the intimin antibody, should also be detectable with the Strep-tag antibody, because the tag is located at the very C terminus of the protein. To test this assumption, we reprobed whole cell lysates of Int WT-Strep and IntHA453-Strep (used in Fig. 4*A*) with antibodies directed against the Strep-tag. PK treatment of bacteria expressing Int WT-Strep leads to degradation of the C-terminal Strep-tag (Fig. 4*D, left*) and additionally results in a loss of fluorescence signal at the bacterial surface (Fig. 4*D, right*). In contrast, the PK fragment arising after proteolysis of IntHA453-Strep was detectable with the Strep-tag antibody (Fig. 4*D, left; labeled* with an *asterisk*). This finding confirmed our hypothesis that the PK fragment comprises the most C-terminal part of the intimin passenger domain. In summary, insertion of the tandem HA tag at position 453 results in destabilization of the intimin passenger domain and renders the protein accessible to PK. However, the PK fragment that is generated is protected from further degradation and obviously inaccessible to antibody binding without permeabilization of the outer membrane.

The ~55-kDa PK Fragment Is Localized in the Periplasm—Proteinase K treatment of bacteria expressing IntHA453 leads to the formation of a ~55-kDa intimin fragment, which can be recognized by Western blot analysis with the intimin as well as
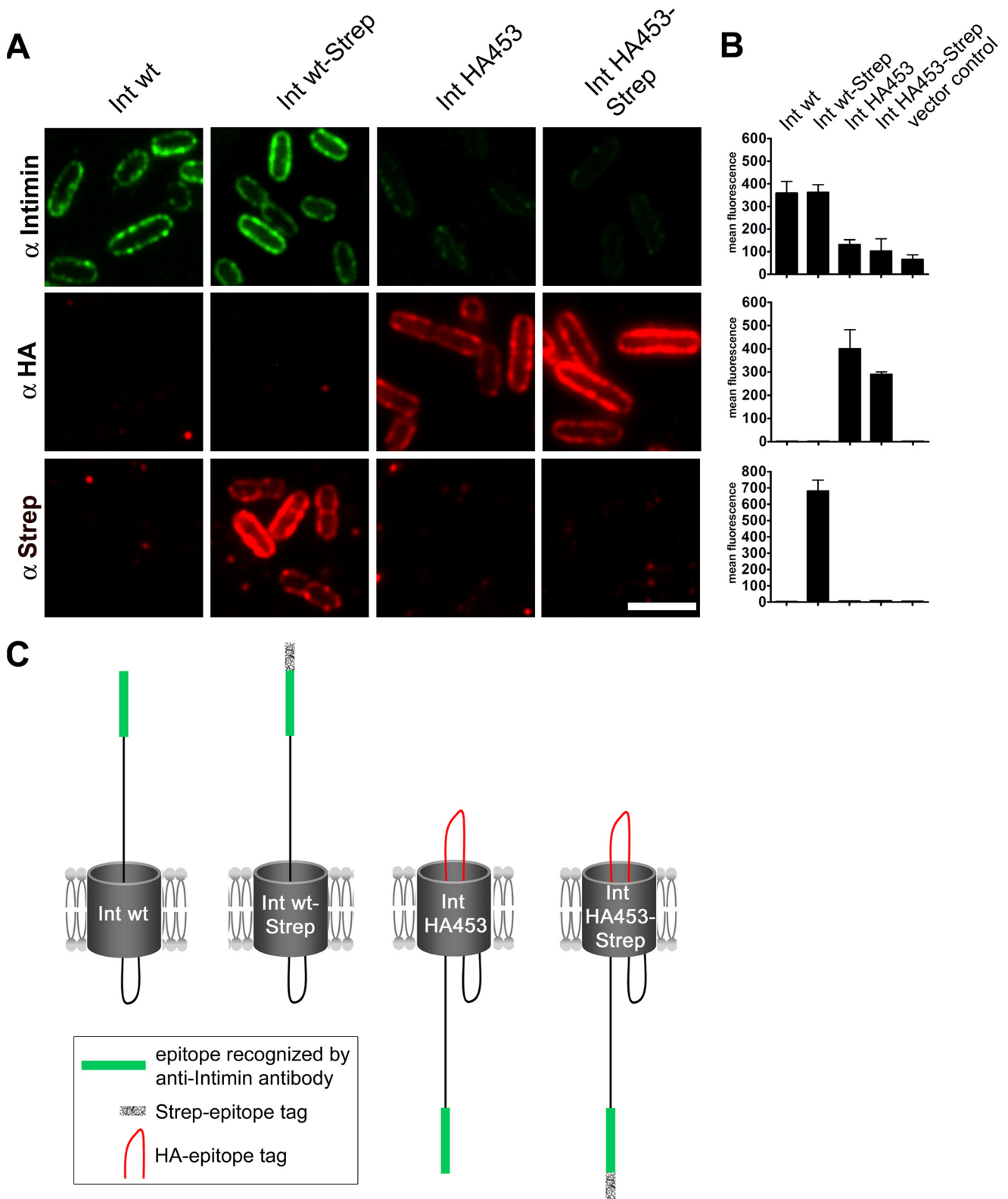
FIGURE 3. **Insertion of a HA tag at position 453 of *E. coli* O127:H6 E2348/69 intimin results in a stalled autotransport intermediate.** *A*, immunofluorescence staining of *E. coli* BL21(DE3)omp2 expressing intimin WT and intimin mutants. Bacteria were fixed and incubated with either intimin antibody recognizing the C terminus, anti-HA tag antibody, or anti-Strep-tag antibody. *Scale bar*, 2 μm. *B*, flow cytometry analysis. Surface exposure of the binding sites for intimin, HA tag, and Strep antibodies was assessed and plotted in mean fluorescence intensity for the indicated constructs, which were expressed in *E. coli* BL21(DE3)omp2. *C*, schematic illustration of the analyzed intimin constructs. The binding site for the intimin antibody at the C terminus of the protein is marked in *green*, and the Strep-tag is *colored blue*. The HA tag that causes the stalled phenotype is *labeled* in *red*. The *bars* show the mean and *error bars* denote the S.D. from three individual measurements.
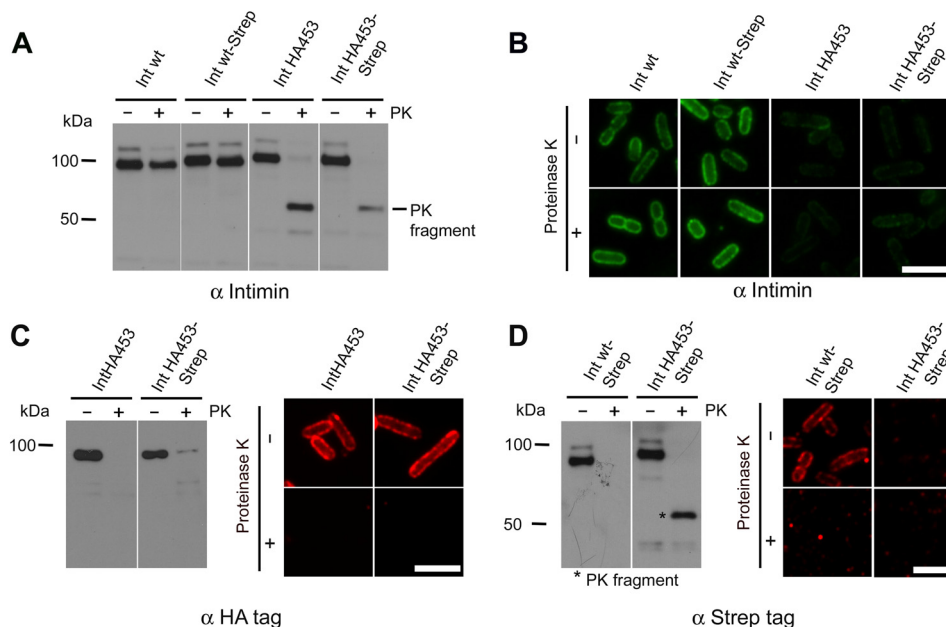
FIGURE 4. PK digestion of intimin mutants expressed in *E. coli* leads to the release of a protected C-terminal fragment. *A*, formation of a ∼55-kDa PK fragment. Bacteria expressing Int WT, IntHA453, and Strep-tagged variants were treated with PK for 30 min. After the addition of PMSF as protease inhibitor, whole cell lysates were subjected to SDS-PAGE, and Western blot analysis with anti-intimin antibody was performed. The generated PK fragment is depicted and only visible for IntHA453 mutants. *B*, immunofluorescence staining of PK-treated bacteria. Bacteria from *A* were labeled with anti-intimin antibody after or without treatment with PK. *C*, the HA tag is cleaved by PK. IntHA453 and IntHA453-Strep samples from *A* were analyzed by Western blot and immunofluorescence-immunodetected with anti-HA tag antibody. Outer membrane staining was only observed for untreated bacteria. *D*, the PK fragment can be recognized by C-terminal Strep-tag. Strep-tag of Int WT-Strep was cleaved after the addition of PK, whereas treatment of IntHA453-Strep resulted in the formation of the protected ∼55-kDa fragment, which can be detected with anti-Strep-tag antibody in Western blot analysis. All *scale bars*, 2 μm.

the Strep-tag antibody (Fig. 4, *A* and *D*). However, because we analyzed whole cell lysates, we were not able to discern whether the fragment might be released into the supernatant or if it was still associated with the bacteria (which would be the case if the fragment resides in the periplasm). To resolve this question, we again expressed IntHA453-Strep in *E. coli* BL21(DE3)omp2 and treated the bacteria with PK. Bacteria expressing Int WT-Strep served as control. Afterward, we separated a pellet fraction containing insoluble material and a supernatant containing soluble proteins. Here, Int WT-Strep, which is inaccessible to PK, was found exclusively in the pellet fraction (Fig. 5*A*). However, the PK fragment was solely found in the pellet fraction and could not be detected in the supernatant (Fig. 5*A*). This indicates that the PK fragment is not quantitatively released into the supernatant but somehow stays associated with the bacteria.

To analyze the localization of the PK fragment in more detail, we additionally performed subcellular fractionation of bacteria expressing Int WT-Strep or IntHA453-Strep after treatment with PK. We separated the cytosolic from the periplasmic and the membrane fraction. In contrast to Int WT-Strep, which is exclusively found in the membrane fraction in its full length, IntHA453 is cleaved, and the major fraction of the PK fragment co-purified with the periplasmic fraction, with another portion found in the membrane fraction (Fig. 5*B*). Untreated whole cell lysates served as an input control. The purity of the subcellular fractions was analyzed by Western blots using antibodies recognizing marker proteins of the respective fractions: DnaK (cytosolic chaperone), SurA (periplasmic chaperone), and BamA (integral outer membrane protein). Taken together, these results support the idea of a stalled autotransport intermediate

adopting a topology as shown in Fig. 3*C*. Here, the passenger domain is cleaved off of the β-barrel domain upon PK treatment. However, it is not released into the supernatant but stays in the periplasm and is protected against further degradation.

The IntHA453 Passenger Domain Is Stalled in a Hairpin Conformation—To test whether inverse (Ve) autotransporters adapt a similar hairpin conformation as discussed for the initiation of Va (13) and Vc (34) autotransport, we expressed Int WT, Int WT-Strep, IntHA453, and IntHA453-Strep in *E. coli* and performed immunofluorescence microscopy. Native bacterial cells were treated with Triton X-100 to permeabilize the outer membrane, or we omitted the permeabilization step. After that, bacteria were incubated with antibodies directed against the C-terminally attached Strep-tag. As shown in Fig. 6, the Strep antibody did not produce any nonspecific signal with bacteria expressing Int WT or IntHA453, irrespective of the treatment with Triton X-100. However, staining of bacteria expressing Int WT-Strep resulted in a ring-shaped peripheral fluorescence even without permeabilization. Permeabilized cells showed comparable outer membrane staining. In contrast to this, using bacteria expressing IntHA453-Strep, the Strep-tag was detectable only if the outer membrane was permeabilized and allowed the antibodies to enter the periplasmic space (Fig. 6). Bacteria expressing IntHA453 did not give a fluorescence signal, demonstrating that the signal we obtained with IntHA453-Strep is not due to nonspecific binding of the anti-Strep antibody to other periplasmic content. In summary, our data obtained by immunofluorescence staining as well as by treatment of bacteria with PK clearly demonstrate that the passenger domain translocation of the IntHA453 is stalled in a hairpin conformation at a point where the N-terminal part of
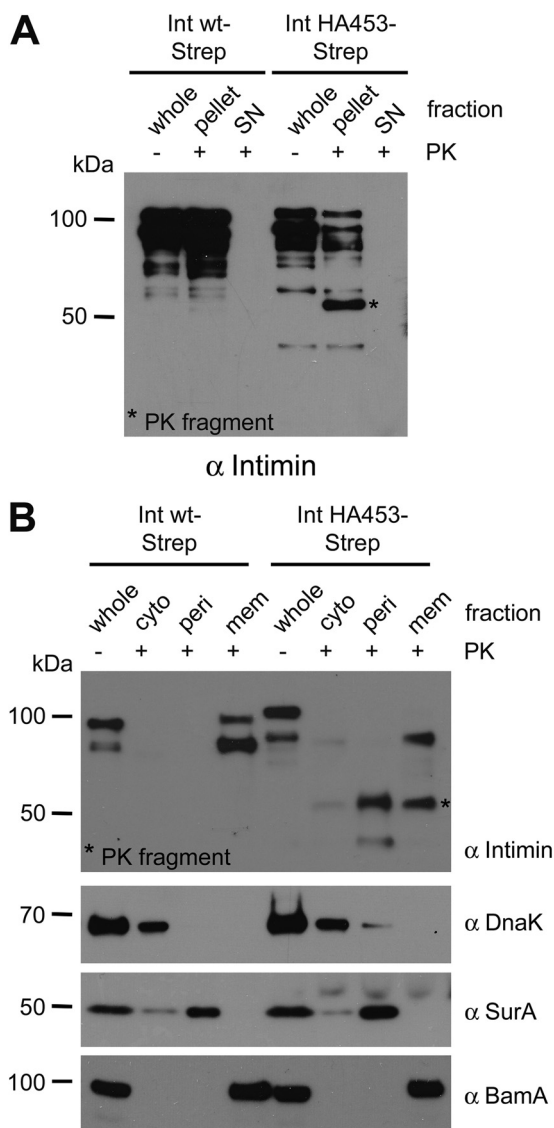
A

α Intimin

B

FIGURE 5. **The protected PK fragment is localized in the periplasm.** *A*, *E. coli* BL21(DE3)omp2 expressing Int WT-Strep or IntHA453-Strep, respectively, was analyzed directly (*whole*) or treated with PK. Afterward, bacteria were centrifuged, and the pellet as well as the supernatant (*SN*) fractions were analyzed by SDS-PAGE and Western blotting using anti-intimin antibody. *B*, subcellular fractionation of *E. coli* BL21(DE3)omp2 expressing Int WT-Strep or IntHA453-Strep after PK treatment. Membrane (*Mem*), periplasmic (*Peri*), and cytosolic (*Cyto*) fractions were analyzed by SDS-PAGE and Western blot with antibodies directed against intimin. BamA (an outer membrane protein), SurA (a periplasmic protein), and DnaK (a cytosolic protein) were used as controls showing the purity of the different fractions.

the passenger (comprising the HA tag) is already surface-exposed, whereas the C terminus is still located in the periplasm.

IntHA453 Copurifies with Components of the β-Barrel Assembly Machinery and the Periplasmic Chaperone SurA after Chemical Cross-linking—Insertion of intimin into the outer membrane of *E. coli* depends on BamA, and it has been shown that the loss of SurA leads to an accumulation of the membrane anchor domain of intimin in the periplasm (15). We have reported previously that invasin, an inverse autotransporter adhesin of *Yersinia enterocolitica*, is no longer inserted into the outer membrane under either BamA depletion or SurA deletion conditions. In our experimental setting, the periplasmic
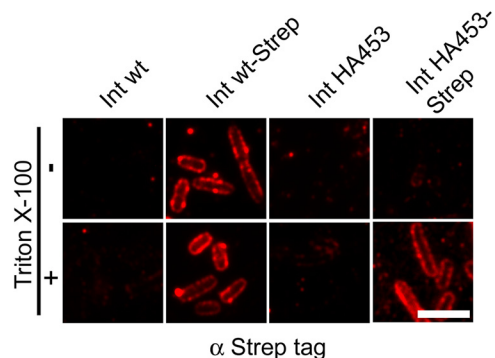

α Strep tag

FIGURE 6. **Immunofluorescence staining of C-terminally Strep-tagged IntHA453 AT intermediate indicates a hairpin conformation of the passenger domain.** Int WT or IntHA453 as well as Strep-tagged variants were expressed in *E. coli* BL21(DE3)omp2. Bacterial outer membrane was permeabilized (*bottom*) or not (*top*) with Triton X-100 prior to staining with anti-Strep-tag primary antibody. *Scale bar*, 5 μm.

chaperone-protease DegP procured the complete degradation of invasin within the periplasm. As a result, the protein was no longer detectable in whole cell lysates (8). In the present study, we wanted to find out whether *in vivo* intimin directly interacts with the periplasmic chaperone SurA and also the β-barrel assembly machinery during its biogenesis. Moreover, we were interested to find out whether these interactions are somehow altered in the stalled autotransporter mutant IntHA453-Strep. To do so, we used DSP, a thiol-cleavable, membrane-permeant, and amine-reactive cross-linker. After cross-linking and solubilization with detergent, we enriched proteins carrying the Strep-tag (and proteins cross-linked to those) by affinity purification using streptavidin-coated beads. The resulting eluates were heated in the presence of dithiothreitol (DTT)-containing Laemmli buffer to reduce the disulfide bond in the spacer arm of DSP and thereby disrupt the cross-links. Finally, all samples were analyzed by SDS-PAGE and Western blot. As a negative control, we included bacteria harboring an empty pASK-IBA2 vector. As shown by Western blot using the anti-intimin antibody, both Int WT-Strep and IntHA453-Strep were recovered well from the solubilized membrane fractions, with the enrichment of Int WT-Strep being slightly more efficient (Fig. 7A). Treatment of the samples with DSP did not significantly affect the efficiency of enrichment of Int WT-Strep or IntHA453-Strep via the Strep-tag. Next we analyzed the identical samples for the presence of BamA and periplasmic chaperones. Without DSP, neither BamA nor periplasmic chaperones copurified with Int WT-Strep, whereas the addition of DSP led to cross-linking of Int WT-Strep to BamA as well as to the chaperones Skp and SurA. Furthermore, we could detect all other BAM complex proteins (BamB, BamC, BamD, and BamE) in samples where BamA was cross-linked.

Whereas the periplasmic chaperone Skp did not reveal enhanced cross-linking to the stalled autotransport intermediate IntHA453-Strep, much more SurA was cross-linked to the stalled mutant compared with Int WT-Strep. This is in accordance with previous data, which showed a specialized role for SurA in passenger domain secretion, whereas Skp has a role only at the early stage of β-barrel assembly. However, the barrel seems to be already folded and assembled for both Int WT and IntHA453 mutants, making an interaction with Skp unlikely at this stage. Moreover,
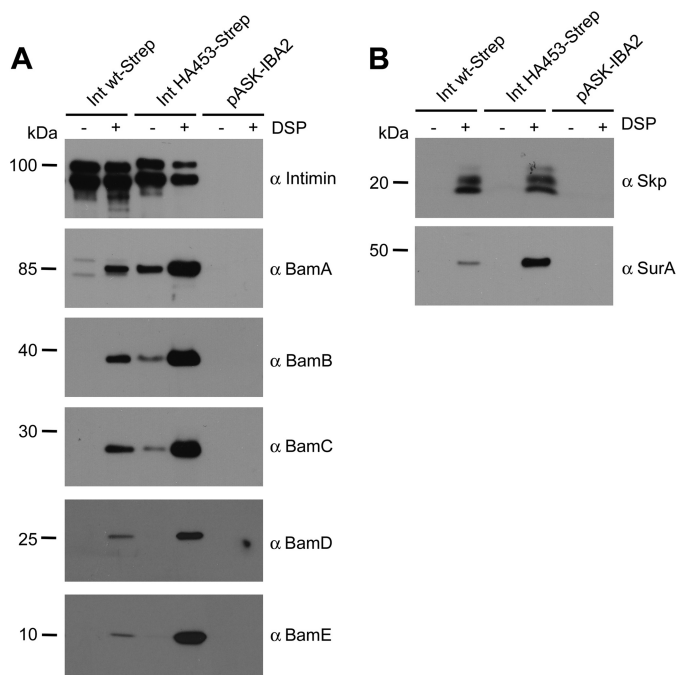
FIGURE 7. **Stalled translocation of the passenger domain allows the identification of transient interaction partners.** *A*, interaction with BAM complex components; *B*, periplasmic chaperones. Bacteria expressing Int WT-Strep or IntHA453-Strep were either incubated with the membrane-permeable cross-linker DSP (+) or left untreated (−). Afterward, outer membrane fractions were isolated, outer membrane proteins were solubilized with *n*-dodecyl β-D-maltoside and Strep-tagged intimin was purified with streptavidin beads. Proteins were eluted from the beads with desthiobiotin and analyzed by Western blot analysis.

the interaction with BamA varied significantly; for IntHA453-Strep, an interaction to BamA was visible already without adding a cross-linker, although such a contact between BamA and a substrate protein like intimin is expected to be very transient. The addition of DSP enhanced the amount of copurified BamA with IntHA453-Strep drastically and also the levels of immunoprecipitated BamB–E. *E. coli* cells harboring only the empty vector pASK-IBA2 served as negative controls for the immunoprecipitation and confirmed the specificity of the antibodies used. To rule out the possibility that the high protein levels of SurA and the BAM complex components cross-linked to IntHA453-Strep were only due to up-regulation of the corresponding genes, we analyzed the expression in whole cell lysates. The steady state levels of the periplasmic chaperones Skp, DegP, and SurA as well as the BAM complex components BamA–E are comparable, independent of which intimin construct was expressed heterologously (Fig. 8).

In summary, our cross-linking data confirm the idea of a stalled autotransport intermediate. Although interactions between outer membrane proteins like intimin with periplasmic chaperones and the BAM complex are very short lived, the addition of DSP can also trap such transient protein-protein contacts. Because the biogenesis of the stalled autotransport intermediate is not completed yet, IntHA453-Strep is still in contact with chaperones and the BAM complex as Int WT-Strep, attempting to facilitate export of the passenger domain to the cell surface and thus to complete protein biogenesis.
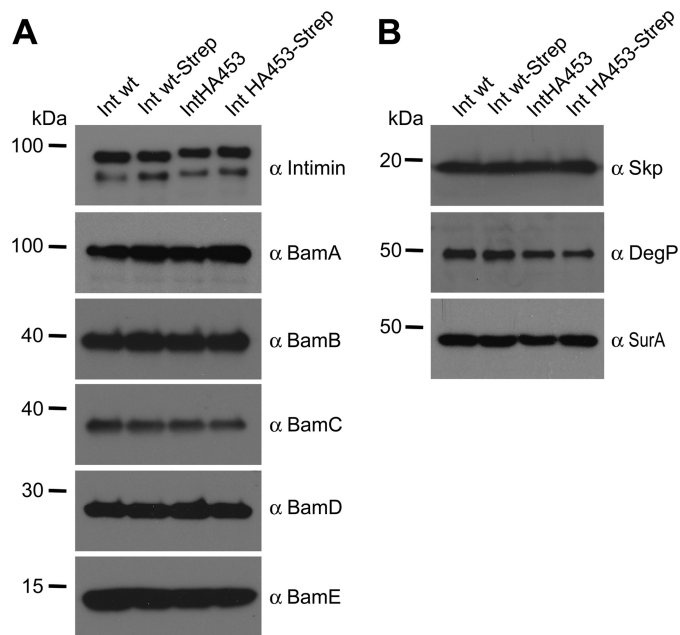

FIGURE 8. **Protein expression levels of BAM complex components and periplasmic chaperones.** *A*, whole cell lysates of *E. coli* BL21(DE3)omp2 expressing Int WT or intimin variants were analyzed for the expression of BAM complex components BamA–BamE. Samples were taken 2 h after the start of intimin protein expression. *B*, protein levels of the periplasmic chaperones Skp, DegP, and SurA in whole cell lysates.

DISCUSSION

E. coli Intimin is a prototypical inverse autotransporter, also called the type Ve secretion system (2, 8). By introducing an HA tag after position 453 in intimin, we have produced a mutant of an inverse autotransporter that is stalled in autotransport. We were able to show that the β-barrel domain is properly inserted in the outer membrane just as in the wild type situation and is folded according to gel shift assays. In contrast, the passenger domain is not located on the cell surface in the mutant, because only the introduced HA tag can be stained with antibodies in unpermeabilized cells, whereas the antibodies specific to the C terminus of the passenger only yield a (periplasmic) fluorescence signal after cell permeabilization with detergent. The stalled autotransporter interacts both with BamA and with the periplasmic chaperone SurA, shown by cross-linking experiments and in accordance with data on type Va autotransporters, where SurA has a special role in passenger secretion (35). The massive decoration with SurA suggests an unfolded conformation of the passenger but at the same time might explain why the protein is protected from proteolysis. It seems that the stalled autotransporter does not trigger the periplasmic stress response under the conditions used in this work (Fig. 8). This is corroborated by the fact that bacteria expressing the stalled autotransporter have neither a growth defect nor an outer membrane protein profile that is significantly changed compared with bacteria expressing the wild type intimin (Fig. 9).

It is widely accepted that autotransport proceeds through the transmembrane β-barrel of the translocation domain via a hairpin intermediate (18, 36) and that this is true for all type V secretion systems with the possible exception of two-partner
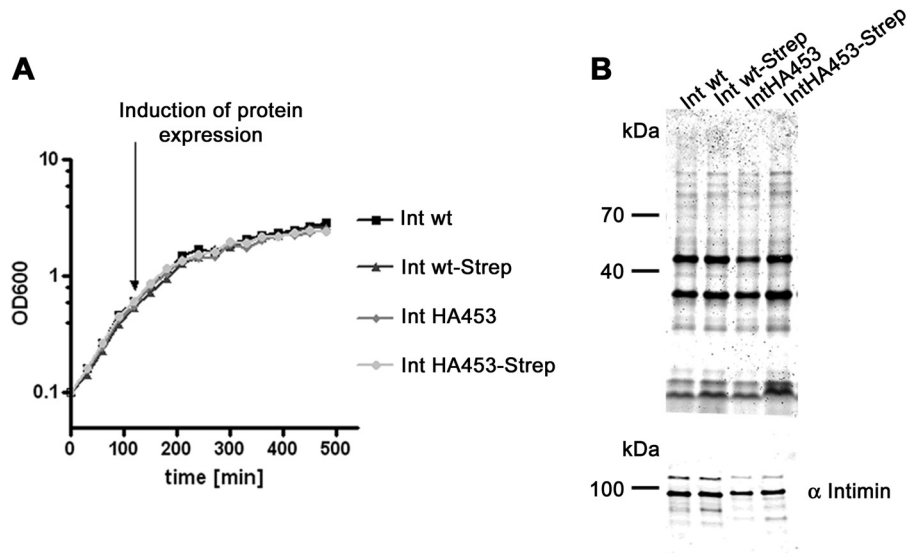
FIGURE 9. **Growth and outer membrane protein profile of bacteria overexpressing IntHA453-Strep.** *A*, expression of the stalled autotransporter does not produce a growth phenotype in bacteria grown at 27 °C. *B*, Coomassie gel and Western blot with anti-intimin antibodies. The outer membrane protein profile remains unchanged upon overexpression of the stalled autotransporter. Expression levels of Int WT, Int WT-Strep, IntHA453, and IntHA453-Strep are comparable.
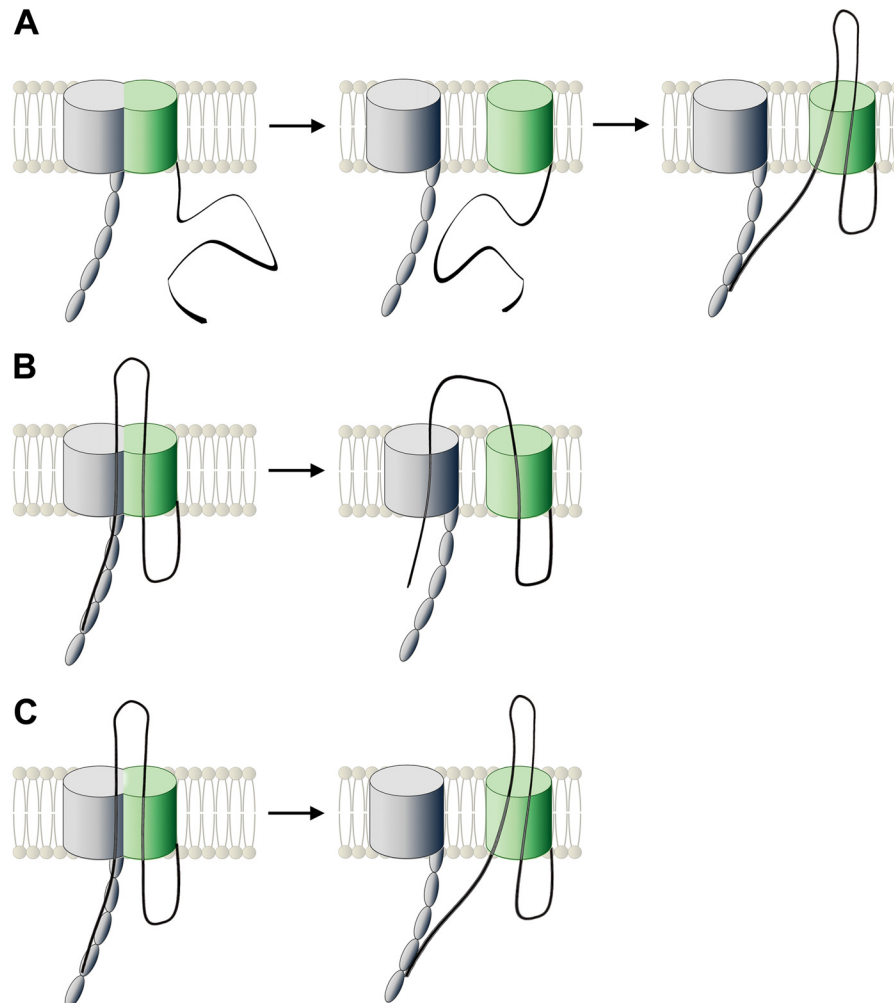

FIGURE 10. **Possible scenarios explaining our findings.** *A*, during the first step of biogenesis, the intimin barrel and the BamA β-barrel build a hybrid barrel from which the intimin barrel buds off into the OM. Then autotransport of the passenger is initiated and is halted due to the presence of the HA tag in a hairpin conformation. Direct contact with BamA at this stage is maintained either via interaction of the passenger with POTRA domain(s) or via the folded β-barrels. *B* and *C*, intimin biogenesis is initiated by the formation of a hybrid barrel with BamA. At this hybrid barrel stage, the hairpin is inserted. Budding of the intimin barrel can lead to two outcomes; the passenger stays in the BamA-barrel and mediates contact to the barrel wall (*B*), or the passenger ends up in the intimin barrel (*C*). Contact with BamA is then mediated either via the POTRA domain(s) or by interaction of the intimin and the BamA β-barrel domains.

secretion (type Vb), where the passenger might also be threaded through the N terminus first (37). Thus, the only explanation for the labeling results where the HA tag is on the cell surface while the rest of the passenger remains in the periplasm is the formation of a hairpin intermediate (Fig. 3C). For classical autotransporters (type Va), it has been suggested that β-barrel insertion and initiation of hairpin formation are coupled and that possibly the barrel is not fully formed when autotransport starts (23, 35, 38). Our data on the type Ve autotransporter intimin show a presumably folded barrel with a stalled hairpin, not necessarily contradicting a simultaneous insertion of barrel and hairpin into the membrane but strongly suggesting that the rest of the autotransport process proceeds with a fully formed barrel present.

The BAM complex is the protein complex that facilitates the membrane insertion and folding of practically all transmembrane β-barrel proteins into the Gram-negative bacterial outer membrane. It is an essential outer membrane component, albeit transmembrane β-barrel proteins readily insert and fold into lipid bilayers *in vitro* completely autonomously (39). Thus, the essential role of the BAM complex in the cell is presumably the lowering of the activation energy for membrane insertion and thus the improvement of insertion kinetics, to avoid accumulation of unfolded proteins in the periplasm. In addition, the POTRA domains of BamA have been shown to act as chaperones, interacting with amphiphatic β-strands (40). The BAM complex is also necessary for *in vivo* insertion of autotransporters that have the same characteristics and the same C-terminal insertion signal as other transmembrane β-barrel proteins (41, 42). The direct involvement of the BAM complex in the biogenesis of autotransporters has been shown in detail for type Va (23, 35, 43) and the trimeric Vc (44) secretion systems as well as for inverse autotransporters (Ve) (8). If and how the BAM complex is also important for hairpin formation is unclear. Recent structural and functional data on the BAM complex suggest that a hybrid barrel is formed between the BamA barrel and the substrate (45– 48). From this intermediate, the substrate barrel is then released in a process that can be described as "budding." Note that our data show a presumably folded barrel in the membrane for the stalled intimin autotransport mutant, strongly suggesting that this budding is completed, whereas autotransport is not. Several scenarios are conceivable that would explain the observed interaction of the mutant with BamA (Fig. 10). (i) The barrel is formed with the help of BamA, but autotransport (and even hairpin formation) is only initiated afterward. This is somewhat in contrast to observations for type Va autotransporters, where barrel insertion and hairpin formation are thought to be coupled (22, 23) (Fig. 10A). (ii) The barrel is formed, and during the hybrid barrel stage, the hairpin is inserted. This can then lead to two different outcomes; one end can stay in the BamA barrel (Fig. 10B), or both ends of the hairpin can end up in the autotransporter barrel (Fig. 10C). In all three cases, the (stalled) passenger domain could still interact with the POTRA domains of BamA, and in some of the cases possibly also with other parts of BamA (*e.g.* with the inside of the BamA barrel), which would explain the crosslinking data presented in this work. Much more detailed interaction studies will be necessary to elucidate the exact sequence of events in autotransport.

It is worth noting that the trimeric autotransporters also depend on BamA for membrane insertion and also seem to form hairpin intermediates (34, 44, 49). It is hard to conceive how three hairpins could be formed and how three parts of a transmembrane β-barrel could be assembled and inserted simultaneously by one BAM complex, and it is difficult to imagine three individual BAM complexes working in a synchronous fashion. The current challenge in the field of autotransport is thus to determine how universal the hairpin mechanism is for all autotransporters, from Type Va to Type Ve.

REFERENCES

1. Leyton, D. L., Rossiter, A. E., and Henderson, I. R. (2012) From self sufficiency to dependence: mechanisms and factors important for autotransporter biogenesis. *Nat. Rev. Microbiol.* **10,** 213–225

2. Leo, J. C., Grin, I., and Linke, D. (2012) Type V secretion: mechanism(s) of autotransport through the bacterial outer membrane. *Philos. Trans. R. Soc. Lond. B Biol. Sci.* **367,** 1088–1101

3. Pohlner, J., Halter, R., Beyreuther, K., and Meyer, T. F. (1987) Gene structure and extracellular secretion of *Neisseria gonorrhoeae* IgA protease. *Nature* **325,** 458–462

4. van Ulsen, P., van Alphen, L., ten Hove, J., Fransen, F., van der Ley, P., and Tommassen, J. (2003) A Neisserial autotransporter NalP modulating the processing of other autotransporters. *Mol. Microbiol.* **50,** 1017–1030

5. Linke, D., Riess, T., Autenrieth, I. B., Lupas, A., and Kempf, V. A. (2006) Trimeric autotransporter adhesins: variable structure, common function. *Trends Microbiol.* **14,** 264–270

6. Jacob-Dubuisson, F., Locht, C., and Antoine, R. (2001) Two-partner secretion in Gram-negative bacteria: a thrifty, specific pathway for large virulence proteins. *Mol. Microbiol.* **40,** 306–313

7. Salacha, R., Kovacić, F., Brochier-Armanet, C., Wilhelm, S., Tommassen, J., Filloux, A., Voulhoux, R., and Bleves, S. (2010) The *Pseudomonas aeruginosa* patatin-like protein PlpD is the archetype of a novel Type V secretion system. *Environ. Microbiol.* **12,** 1498–1512

8. Oberhettinger, P., Schütz, M., Leo, J. C., Heinz, N., Berger, J., Autenrieth, I. B., and Linke, D. (2012) Intimin and invasin export their C-terminus to the bacterial cell surface using an inverse mechanism compared to classical autotransport. *PLoS One* **7,** e47069

9. Grassl, G. A., Bohn, E., Müller, Y., Bühler, O. T., and Autenrieth, I. B. (2003) Interaction of *Yersinia enterocolitica* with epithelial cells: invasin beyond invasion. *Int. J. Med. Microbiol.* **293,** 41–54

10. Frankel, G., Phillips, A. D., Rosenshine, I., Dougan, G., Kaper, J. B., and Knutton, S. (1998) Enteropathogenic and enterohaemorrhagic *Escherichia coli*: more subversive elements. *Mol. Microbiol.* **30,** 911–921

11. Jerse, A. E., Yu, J., Tall, B. D., and Kaper, J. B. (1990) A genetic locus of enteropathogenic *Escherichia coli* necessary for the production of attaching and effacing lesions on tissue culture cells. *Proc. Natl. Acad. Sci. U.S.A.* **87,** 7839–7843

12. Touzé, T., Hayward, R. D., Eswaran, J., Leong, J. M., and Koronakis, V. (2004) Self-association of EPEC intimin mediated by the β-barrel-containing anchor domain: a role in clustering of the Tir receptor. *Mol. Microbiol.* **51,** 73–87

13. Tsai, J. C., Yen, M. R., Castillo, R., Leyton, D. L., Henderson, I. R., and Saier, M. H., Jr. (2010) The bacterial intimins and invasins: a large and novel family of secreted proteins. *PLoS One* **5,** e14403

14. Leo, J. C., Oberhettinger, P., Chaubey, M., Schütz, M., Kühner, D., Bertsche, U., Schwarz, H., Götz, F., Autenrieth, I. B., Coles, M., and Linke, D. (2014) The Intimin periplasmic domain mediates dimerisation and binding to peptidoglycan. *Mol. Microbiol.* 10.1111/mmi.12840

15. Bodelón, G., Marín, E., and Fernández, L. A. (2009) Role of periplasmic

chaperones and BamA (YaeT/Omp85) in folding and secretion of intimin from enteropathogenic *Escherichia coli* strains. *J. Bacteriol.* **191,** 5169–5179

16. Adams, T. M., Wentzel, A., and Kolmar, H. (2005) Intimin-mediated export of passenger proteins requires maintenance of a translocation-competent conformation. *J. Bacteriol.* **187,** 522–533

17. Maurer, J., Jose, J., and Meyer, T. F. (1999) Characterization of the essential transport function of the AIDA-I autotransporter and evidence supporting structural predictions. *J. Bacteriol.* **181,** 7014–7020

18. Junker, M., Besingi, R. N., and Clark, P. L. (2009) Vectorial transport and folding of an autotransporter virulence protein during outer membrane secretion. *Mol. Microbiol.* **71,** 1323–1332

19. Peterson, J. H., Tian, P., Ieva, R., Dautin, N., and Bernstein, H. D. (2010) Secretion of a bacterial virulence factor is driven by the folding of a C-terminal segment. *Proc. Natl. Acad. Sci. U.S.A.* **107,** 17739–17744

20. Kang'ethe, W., and Bernstein, H. D. (2013) Stepwise folding of an autotransporter passenger domain is not essential for its secretion. *J. Biol. Chem.* **288,** 35028–35038

21. Kang'ethe, W., and Bernstein, H. D. (2013) Charge-dependent secretion of an intrinsically disordered protein via the autotransporter pathway. *Proc. Natl. Acad. Sci. U.S.A.* **110,** E4246–E4255

22. Ieva, R., and Bernstein, H. D. (2009) Interaction of an autotransporter passenger domain with BamA during its translocation across the bacterial outer membrane. *Proc. Natl. Acad. Sci. U.S.A.* **106,** 19120–19125

23. Sauri, A., Soprova, Z., Wickström, D., de Gier, J. W., Van der Schors, R. C., Smit, A. B., Jong, W. S., and Luirink, J. (2009) The Bam (Omp85) complex is involved in secretion of the autotransporter haemoglobin protease. *Microbiology* **155,** 3982–3991

24. Jong, W. S., ten Hagen-Jongman, C. M., den Blaauwen, T., Slotboom, D. J., Tame, J. R., Wickström, D., de Gier, J. W., Otto, B. R., and Luirink, J. (2007) Limited tolerance towards folded elements during secretion of the autotransporter Hbp. *Mol. Microbiol.* **63,** 1524–1536

25. Fairman, J. W., Dautin, N., Wojtowicz, D., Liu, W., Noinaj, N., Barnard, T. J., Udho, E., Przytycka, T. M., Cherezov, V., and Buchanan, S. K. (2012) Crystal structures of the outer membrane domain of intimin and invasin from enterohemorrhagic *E. coli* and enteropathogenic *Y. pseudotuberculosis*. *Structure* **20,** 1233–1243

26. Adu-Bobie, J., Trabulsi, L. R., Carneiro-Sampaio, M. M., Dougan, G., and Frankel, G. (1998) Identification of immunodominant regions within the C-terminal cell binding domain of intimin α and intimin β from enteropathogenic *Escherichia coli*. *Infect. Immun.* **66,** 5643–5649

27. Batchelor, M., Prasannan, S., Daniell, S., Reece, S., Connerton, I., Bloomberg, G., Dougan, G., Frankel, G., and Matthews, S. (2000) Structural basis for recognition of the translocated intimin receptor (Tir) by intimin from enteropathogenic *Escherichia coli*. *EMBO J.* **19,** 2452–2464

28. Grosskinsky, U., Schütz, M., Fritz, M., Schmid, Y., Lamparter, M. C., Szczesny, P., Lupas, A. N., Autenrieth, I. B., and Linke, D. (2007) A conserved glycine residue of trimeric autotransporter domains plays a key role in *Yersinia* adhesin A autotransport. *J. Bacteriol.* **189,** 9011–9019

29. Schütz, M., Weiss, E. M., Schindler, M., Hallström, T., Zipfel, P. F., Linke, D., and Autenrieth, I. B. (2010) Trimer stability of YadA is critical for virulence of *Yersinia enterocolitica*. *Infect. Immun.* **78,** 2677–2690

30. Rosenbusch, J. P. (1974) Characterization of the major envelope protein from *Escherichia coli*: regular arrangement on the peptidoglycan and unusual dodecyl sulfate binding. *J. Biol. Chem.* **249,** 8019–8029

31. Soprova, Z., Sauri, A., van Ulsen, P., Tame, J. R., den Blaauwen, T., Jong, W. S., and Luirink, J. (2010) A conserved aromatic residue in the autochaperone domain of the autotransporter Hbp is critical for initiation of outer membrane translocation. *J. Biol. Chem.* **285,** 38224–38233

32. Kühnel, K., and Diezmann, D. (2011) Crystal structure of the autochaperone region from the *Shigella flexneri* autotransporter IcsA. *J. Bacteriol.* **193,** 2042–2045

33. Oliver, D. C., Huang, G., Nodel, E., Pleasance, S., and Fernandez, R. C. (2003) A conserved region within the *Bordetella pertussis* autotransporter BrkA is necessary for folding of its passenger domain. *Mol. Microbiol.* **47,** 1367–1383

34. Shahid, S. A., Bardiaux, B., Franks, W. T., Krabben, L., Habeck, M., van Rossum, B. J., and Linke, D. (2012) Membrane-protein structure determination by solid-state NMR spectroscopy of microcrystals. *Nat. Methods* **9,** 1212–1217

35. Ieva, R., Tian, P., Peterson, J. H., and Bernstein, H. D. (2011) Sequential and spatially restricted interactions of assembly factors with an autotransporter β domain. *Proc. Natl. Acad. Sci. U.S.A.* **108,** E383–E391

36. Leyton, D. L., Sevastsyanovich, Y. R., Browning, D. F., Rossiter, A. E., Wells, T. J., Fitzpatrick, R. E., Overduin, M., Cunningham, A. F., and Henderson, I. R. (2011) Size and conformation limits to secretion of disulfide-bonded loops in autotransporter proteins. *J. Biol. Chem.* **286,** 42283–42291

37. Jacob-Dubuisson, F., Guérin, J., Baelen, S., and Clantin, B. (2013) Two-partner secretion: as simple as it sounds? *Res. Microbiol.* **164,** 583–595

38. Ieva, R., Skillman, K. M., and Bernstein, H. D. (2008) Incorporation of a polypeptide segment into the β-domain pore during the assembly of a bacterial autotransporter. *Mol. Microbiol.* **67,** 188–201

39. Kleinschmidt, J. H. (2003) Membrane protein folding on the example of outer membrane protein A of *Escherichia coli*. *Cell. Mol. Life Sci.* **60,** 1547–1558

40. Knowles, T. J., Jeeves, M., Bobat, S., Dancea, F., McClelland, D., Palmer, T., Overduin, M., and Henderson, I. R. (2008) Fold and function of polypeptide transport-associated domains responsible for delivering unfolded proteins to membranes. *Mol. Microbiol.* **68,** 1216–1227

41. Remmert, M., Linke, D., Lupas, A. N., and Söding, J. (2009) HHomp: prediction and classification of outer membrane proteins. *Nucleic Acids Res.* **37,** W446–W451

42. Paramasivam, N., Habeck, M., and Linke, D. (2012) Is the C-terminal insertional signal in Gram-negative bacterial outer membrane proteins species-specific or not? *BMC Genomics* **13,** 510

43. Jain, S., and Goldberg, M. B. (2007) Requirement for YaeT in the outer membrane assembly of autotransporter proteins. *J. Bacteriol.* **189,** 5393–5398

44. Lehr, U., Schütz, M., Oberhettinger, P., Ruiz-Perez, F., Donald, J. W., Palmer, T., Linke, D., Henderson, I. R., and Autenrieth, I. B. (2010) C-terminal amino acid residues of the trimeric autotransporter adhesin YadA of *Yersinia enterocolitica* are decisive for its recognition and assembly by BamA. *Mol. Microbiol.* **78,** 932–946

45. Noinaj, N., Fairman, J. W., and Buchanan, S. K. (2011) The crystal structure of BamB suggests interactions with BamA and its role within the BAM complex. *J. Mol. Biol.* **407,** 248–260

46. Noinaj, N., Kuszak, A. J., Balusek, C., Gumbart, J. C., and Buchanan, S. K. (2014) Lateral opening and exit pore formation are required for BamA function. *Structure* **22,** 1055–1062

47. Noinaj, N., Kuszak, A. J., Gumbart, J. C., Lukacik, P., Chang, H., Easley, N. C., Lithgow, T., and Buchanan, S. K. (2013) Structural insight into the biogenesis of β-barrel membrane proteins. *Nature* **501,** 385–390

48. Albrecht, R., Schütz, M., Oberhettinger, P., Faulstich, M., Bermejo, I., Rudel, T., Diederichs, K., and Zeth, K. (2014) Structure of BamA, an essential factor in outer membrane protein biogenesis. *Acta Crystallogr. D Biol. Crystallogr.* **70,** 1779–1789

49. Mikula, K. M., Leo, J. C., Łyskowski, A., Kedracka-Krok, S., Pirog, A., and Goldman, A. (2012) The translocation domain in trimeric autotransporter adhesins is necessary and sufficient for trimerization and autotransportation. *J. Bacteriol.* **194,** 827–838

50. Iguchi, A., Thomson, N. R., Ogura, Y., Saunders, D., Ooka, T., Henderson, I. R., Harris, D., Asadulghani, M., Kurokawa, K., Dean, P., Kenny, B., Quail, M. A., Thurston, S., Dougan, G., Hayashi, T., Parkhill, J., and Frankel, G. (2009) Complete genome sequence and comparative genome analysis of enteropathogenic *Escherichia coli* O127:H6 strain E2348/69. *J. Bacteriol.* **191,** 347–354

51. Prilipov, A., Phale, P. S., Van Gelder, P., Rosenbusch, J. P., and Koebnik, R. (1998) Coupling site-directed mutagenesis with high-level expression: large scale production of mutant porins from *E. coli*. *FEMS Microbiol. Lett.* **163,** 65–72

The Inverse Autotransporter Intimin Exports Its Passenger Domain via a Hairpin Intermediate

Philipp Oberhettinger, Jack C. Leo, Dirk Linke, Ingo B. Autenrieth and Monika S. Schütz

Access the most updated version of this article at doi: 10.1074/jbc.M114.604769

Alerts:
- When this article is cited
- When a correction for this article is posted

Click here to choose from all of JBC's e-mail alerts

This article cites 51 references, 20 of which can be accessed free at
http://www.jbc.org/content/290/3/1837.full.html#ref-list-1